ACS Macro Letters

pubs.acs.org/macroletters Letter

Synergistic Effect of Stretched Bridging Block and Released Packing Frustration Leads to Exotic Nanostructures

Qiong Xie,‡ Yicheng Qiang,‡ Lei Chen,‡ Yueming Xia,‡ and Weihua Li*

Cite This: ACS Macro Lett. 2020, 9, 980−984 Read Online

ACCESS | Metrics & More | Article Recommendations | Supporting Information

ABSTRACT: The self-assembly of amphiphilic macromolecules into various mesocrystals has attracted abiding interest. Although many interesting mesocrystals have been achieved, mesocrystals of a low coordination number (CN) such as simple cubic are rarely reported. Here we purposely design an AB-type multiblock copolymer to target exotic spherical phases of low CNs. Self-consistent field theory reveals that two sophisticated mechanisms are realized in the copolymer, that is, stretched bridging block and released packing frustration, synergistically leading to the formation of three spherical phases with extremely low CNs, including the simple cubic spheres (CN = 6), the cubic diamond spheres (CN = 4), and normally aligned hexagonal-packing spheres (6 < CN < 8) in a considerable parameter region. Moreover, we demonstrate that these exotic phases are hard to be stabilized by either of the two mechanisms individually.

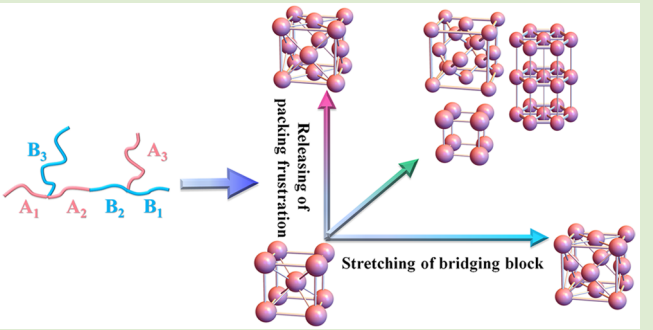

Crystals whose constituents are arranged on periodic crystalline lattices are one class of the most useful materials, and thus, their formation has attracted abiding interest. The fundamental problem of crystal formation is the packing of particles. Natural or conventional crystals are mainly constituted by atoms and ions possessing a lattice constant of subnanometer. An extension of the lattice constant of crystalline structures to the nanoscale or mesoscale should broaden their applications.[1−3]

In recent decades, increasing attention has been paid to fabricating crystalline structures with large lattice constants.[4−8] One direct way is to substitute nanoparticles for atoms or molecules, making nanocrystals with a lattice constant ranging from nanometers to hundreds of nanometers.[9] Alternatively, crystalline structures at the mesoscale can be made from the self-assembly of various amphiphilic macromolecules (e.g., block copolymers,[10−13] amphiphilic liquid crystals,[14−16] and giant surfactants[17−19]). Self-assembled spherical domains as "artificial macromolecular atoms" (AMAs)[20] are composed of dozens or even hundreds of macromolecules.

Conventional crystals and soft mesocrystals possess the common crystalline lattices that are subject to 230 space groups. Interestingly, some crystalline lattices are common, such as face-centered-cubic (FCC) and body-centered-cubic (BCC), but some are really rare.[21] One simple but rare crystalline structure is the simple cubic (SC). One important characteristic of the crystalline lattice is the particle packing factor (denoted by $\overline{\phi}$). Apparently, the SC lattice has a much lower packing factor ($\overline{\phi}$ = 0.524) than that of FCC ($\overline{\phi}$ = 0.740) and BCC ($\overline{\phi}$ = 0.680). Another characteristic parameter, the coordination number of SC (CN = 6), is also much lower than that of FCC (CN = 12) and BCC (CN = 12.5). Another interesting mesocrystal of low CN is the diamond lattice of spheres (DS, CN = 4)[22] that, as a photonic crystal, can generate a complete band gap.[23]

Among macromolecular constituents of mesocrystals, a block copolymer (BCP) is of particular interest due to a few advantages.[10,24,25] First of all, the self-assembly of block copolymers can be readily tuned to form various crystalline structures (e.g., spherical phases) by tailoring their architectures and compositions.[12,26−33] Second, the lattice constant of BCP mesocrystals is dictated by the molecular weight and thus can be tuned from dozens to hundreds of nanometers. In addition, many chemical methods have been developed to complex inorganic components with block copolymers, thus, diversifying the properties of block copolymer mesocrystals.[34−37] Therefore, BCP mesocrystals exhibit a promising prospect of applications. However, mesocrystals of low CNs such as SC and DS are rarely reported in BCPs, which limits the application of mesocrystals.

Here we aim to design a new AB-type BCP to target stable spherical phases of low CNs on the basis of self-consistent field

Received: April 23, 2020
Accepted: June 16, 2020

https://dx.doi.org/10.1021/acsmacrolett.0c00313
ACS Macro Lett. 2020, 9, 980−984

theory (SCFT) studies. To make full use of the efficiency of SCFT, we model each block as a Gaussian chain with equal segment length b and density ρ_0.[38,39] Moreover, we concentrate on the variable of BCP architectures. Nevertheless, some useful guiding principles are still needed, otherwise it is still a formidable task to find the desired architecture in the huge library of architectures.[40]

For the self-assembly of BCPs, one of the most critical factors that disfavors crystalline structures of low CNs is the packing frustration.[38] The packing frustration in crystalline structures mainly results from the polyhedral shape of the Wigner−Seitz cell, in which the majority blocks are nonuniformly stretched in order to fill the space uniformly, resulting in a loss of entropy.[41] One way of reducing the nonuniformity of stretching is to deform the A/B interface from circular to approaching the polyhedral shape, which causes nonuniform stretching with the minority blocks as well as a penalty to the interfacial energy.[38] The two contradictory tendencies induce the packing frustration of polymer chains.[28,41] In the SC or DS phase, the packing frustration becomes exceptionally high.

Very recently, an efficient sophisticated mechanism has been proposed to release the packing frustration of BCPs, that is, intramolecular segregation between two different blocks within the same copolymer chain.[42,43] More specifically, the long blocks are favorably distributed to the further space, while the short blocks go to the nearby space. This mechanism releases the extra packing frustration in the FCC morphology and thus makes FCC become stable over the usual BCC phase.[31] On the other hand, there is another mechanism to drive the transition from the crystalline phase of high CN to that of low CN, that is, stretched bridging block spanning a pair of neighboring domains. The main effect of this mechanism is to reduce the domain-to-domain distance and thus to release the stretching of the bridging block by lowering the CN of crystalline lattices.[20,44]

Neither released packing frustration nor stretched bridging block can stabilize the SC or DS phase;[31,44] however, the synergistic effect of the two mechanisms enhances the possibility. Accordingly, we purposely design an AB-type BCP molecule denoted as $(B_T)AB(A_T)$ (Figure 1a), which is composed of an AB diblock copolymer with A/B-block tethered by an extra B/A-block, respectively. The A-block (B-block) is divided by the tethering point into A_1/A_2-blocks (B_1/B_2-blocks), and the tethering block is denoted as the B_3-block (A_3-block). Obviously, this molecule has exchange symmetry with respect to A and B in topology. If A-blocks as a minority self-assemble into discrete domains (Figure 1b), the lengths of three B-blocks can be tuned for them to reach different areas separately, thus, releasing the packing frustration of B-blocks in the matrix. On the other hand, the B_2-block should form a portion of bridging configurations spanning a pair of A-domains, and its stretching degree can be adjusted by changing its relative length for a fixed total length of B-blocks. In brief, both mechanisms of released packing frustration and stretched bridging block can be realized simultaneously in the discrete morphologies of the $(B_T)AB(A_T)$ copolymer.

We consider an incompressible melt of volume V consisting of n identical $(B_T)AB(A_T)$ copolymers, each of which is composed of N segments in total. The number of segments on the six blocks is denoted as $f_{A1}N$, $f_{A2}N$, $f_{A3}N$, $f_{B1}N$, $f_{B2}N$, and $f_{B3}N$, respectively, with $f_{A1} + f_{A2} + f_{A3} = f$ and $f_{B1} + f_{B2} + f_{B3} = f_B = 1 - f$. In the case of $f < 0.5$, the packing frustration mainly

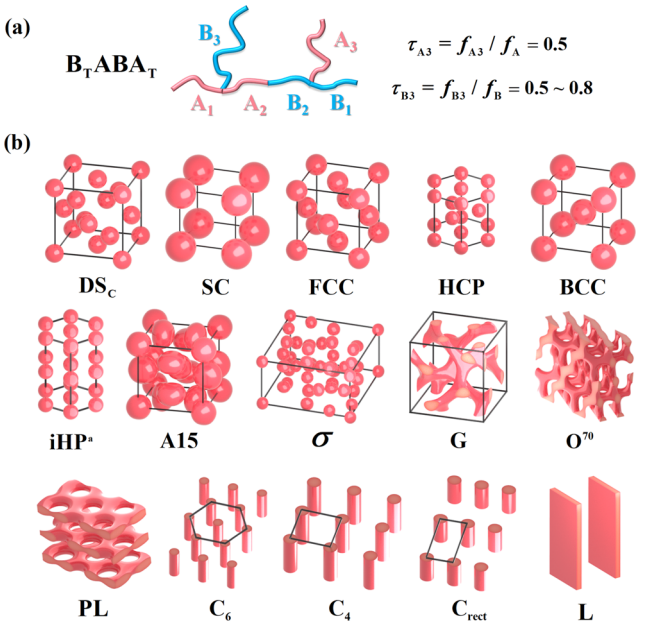

Figure 1. (a) Schematic for considered $(B_T)AB(A_T)$ multiblock copolymer. (b) Density plots of A-domains for considered morphologies.

resulting from the majority B-blocks can be controlled by the relative lengths of B_1 and B_3. On the other hand, the stretching degree of the bridging B_2-block is controlled by f_{B2}. We fix $f_{A1} = f_{A2}$, and introduce $\tau_{A3} = f_{A3}/f$, $\xi = \log(f_{B3}/f_{B1})$ and $\tau_{B2} = f_{B2}/f_B$. Accordingly, the packing frustration and the stretching of bridging block are controlled by ξ and τ_{B2}, respectively. Obviously, $\xi = 0$ gives rise to high packing frustration as equal B_1- and B_3-blocks fill the further and nearby space without any preference; otherwise, larger $|\xi|$ leads to lower packing frustration. The stretching degree of bridging block increases as τ_{B2} decreases. As unequal A_3- and A_1/A_2-blocks favor the formation of spherical domains,[45] we simply choose $\tau_{A3} = 0.5$.

In Figure 2, we present the phase diagram with respect to τ_{B2} and ξ for $\chi N = 100$ and $f = 0.14$. To make the phase diagram reliable, we consider as many candidate phases as possible. The stable ordered phases predicted in this work are listed in Figure

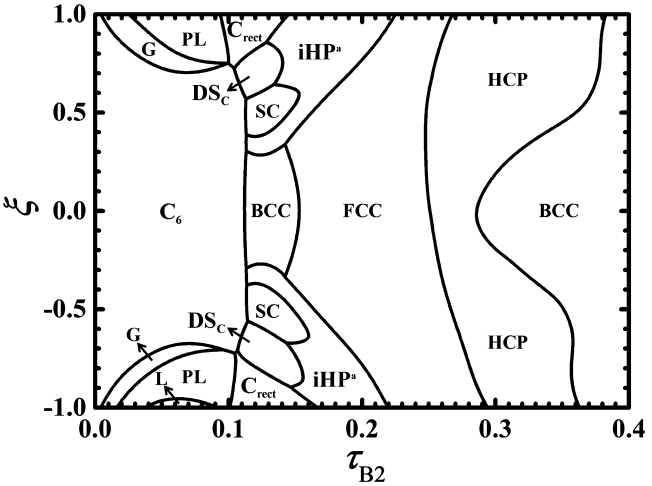

Figure 2. Phase diagram of $(B_T)AB(A_T)$ block copolymer with respect to τ_{B2} and ξ for fixed $\chi N = 100$, $f = 0.14$ and $\tau_{A3} = 0.5$.

https://dx.doi.org/10.1021/acsmacrolett.0c00313
ACS Macro Lett. 2020, 9, 980−984

1b, while those metastable phases are listed in Figure S2. This phase diagram exhibits many surprising features, of which the most remarkable one is the presence of considerable regions of the SC phase and the cubic diamond phase (DS_C), as well as other low-CN phases, such as irregularly layered hexagonal-packing spheres, where all layers are aligned normally (iHP[a]), square cylinders (C_4), and rectangular cylinders (C_{rect}; Figure S3). Note that the hexagonal diamond phase (DS_H)[46] and another hexagonal packing of spheres (iHP) similar to HCP but with enlarged layering distance are found to be metastable. The two cylindrical phases of C_4 and C_{rect} were first reported in a dendritic copolymer by Lee et al.[47] Then, Gao et al. revealed that the low-CN cylinders are stabilized by the mechanism of stretched bridging blocks.[44] However, the effects of the two mechanisms of stretched bridging block and released packing frustration are rarely discussed separately. In the following, we will demonstrate the synergistic effect of the two mechanisms is essential for stabilizing these discrete phases of extremely low CNs.

The main transitions between different spherical phases in Figure 2 are illustrated in Figure 3. Along the path of

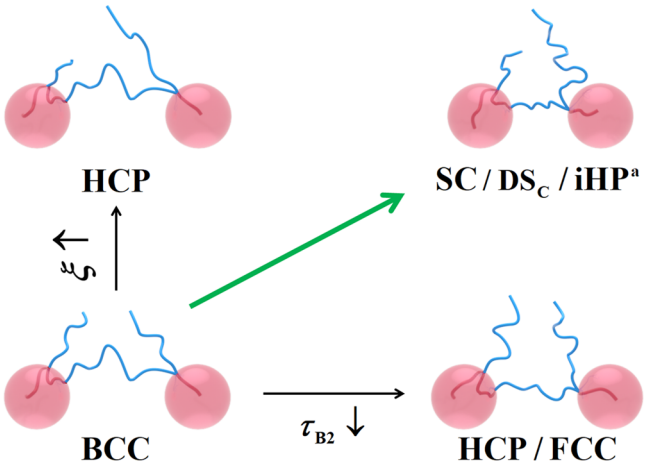

Figure 3. Illustration for the main transitions between different spherical phases in the phase diagram of Figure 2, where a typical bridging configuration spanning a pair of neighboring spheres is plotted.

decreasing τ_{B2} for $\xi = 0$, the stretching of the bridging B_2-block is continuously increased until the bridging configuration is disrupted, while the packing frustration in the case of equal B_1- and B_3-blocks hardly changes. As a result, the transition of spherical phases follows the sequence of BCC → HCP/FCC → BCC. Note that the relative stability between the two spherical phases of HCP and FCC is hard to be explained because of their equal CN and nearly degenerate free energies.[48] When $\tau_{B2} < 0.11$, the bridging configuration of the B_2-block starts to be disrupted, making the interfacial energy more dominant and, thus, driving the transition from BCC to the cylindrical phase (C_6; Figure S4).[44]

In the region of $0.3 < \tau_{B2} < 0.36$, where the bridging B_2-block is not significantly stretched, the transition from BCC to HCP is solely induced by increasing ξ, that is, the effect of released packing frustration (Figure 3). It is interesting to note that the phase diagram is nearly mirror symmetric with respect to the axis of $\xi = 0$. The slight asymmetry originates from the topological asymmetry between B_1- and B_3-blocks. This observation confirms that the releasing effect of packing frustration mainly results from the length difference between B_1- and B_3-blocks, no matter which one is longer. Herein we take the SC phase as an example to illustrate the synergistic effect of the stretched bridging block and the released packing frustration on the formation of these spherical phases with extremely low CNs. Within the stability region of SC centering around $\tau_{B2} \approx 0.13$ and $|\xi| \approx 0.5$, the bridging B_2-block is highly stretched and the length ratio of B_1/B_3-blocks is around 3. The bridging fractions[49,50] of SC and its neighboring phases for $\xi = \log 3$ decline as τ_{B2} decreases due to the increasing stretching (Figure S5). The stretching of B_2-block is evidenced by the aggregation of its midpoint at the center of the line connecting each pair of neighboring spheres (Figure S6), while the lower stretching degree of SC than its competing phases of higher CNs can be seen from its smaller sphere-to-sphere distance (l_0; Figure S7). Moreover, the difference in the bridging fractions between SC and other phases gradually increases as the stretching degree of the B_2-block rises up until most of the bridging configurations are disrupted (Figure S5). The released packing frustration is illustrated by the distinguished distributions of the end points of B_1- and B_3-blocks (Figure S6).

For Gaussian chains, the ratio of their extending distances is about $\sqrt{3}$, close to the ratio between the distances from the cubic center to its face and vertex. Thus, the long and short B_1/B_3-blocks can be locally separated to favorably reach the faces and vertices of the cubic unit, largely releasing the packing frustration of B-blocks within the matrix. As a result, the combined effect of the stretched bridging block and the released packing frustration stabilizes the SC phase. When $|\xi|$ increases further, largely different B_1/B_3-blocks are suitable for filling more nonspherical or noncircular Wigner-Seitz cells, thus, stabilizing DS_C, iHP[a], and C_{rect}. Another surprising transition induced by increasing $|\xi|$ is $C_6 \rightarrow G$ for $\tau_{B2} < 0.1$. This is because the segregation degree increases when B_1/B_3-blocks gradually change from equal to unequal (Figure S8). It is necessary to note that the segregation degree of the hexablock copolymer at $\chi N = 100$ indicated by the A/B-segment distributions of SC is not very high (Figure S9). Moreover, the further transition from G to PL is also induced by the released packing frustration.[42]

As f and χN are two usual control parameters of AB-type copolymers, we construct a two-dimensional phase diagram at the $f-\chi N$ plane in Figure 4 by fixing other parameters: $f_{A1} = f_{A2} = f_{A3}/2 = f/4$, $f_{B1} = f_{B2} = 0.15(1 - f)$ and $f_{B3} = 0.7(1 - f)$. This phase diagram is in striking contrast to previous phase diagrams of AB-type block copolymers, especially the portion at the left side of the lamella.[29] Notably, the region where the BCC phase is usually stable is mainly occupied by three nonclassical phases of SC, iHP[a], and DS_C, except for a very tiny window of BCC at the vicinity of the order−disorder boundary (Figure S10). Similar to the spherical region, there are three nonclassical cylindrical phases in addition to the classical C_6 phase, that is, C_4, C_3, and C_{rect}. The transitions between these spherical and cylindrical phases indicate that their CN, in general, decreases as χN increases. This is because the stretching degree of the bridging block rises up as χN increases, thus, driving the transition of crystalline phases toward the direction of lowering CN.[44] On the other hand, the crystalline phase of lower CN has more favorable interfacial energy.

In addition, it is interesting to note that the phase boundaries are tremendously shifted toward the direction of

https://dx.doi.org/10.1021/acsmacrolett.0c00313
ACS Macro Lett. 2020, 9, 980−984

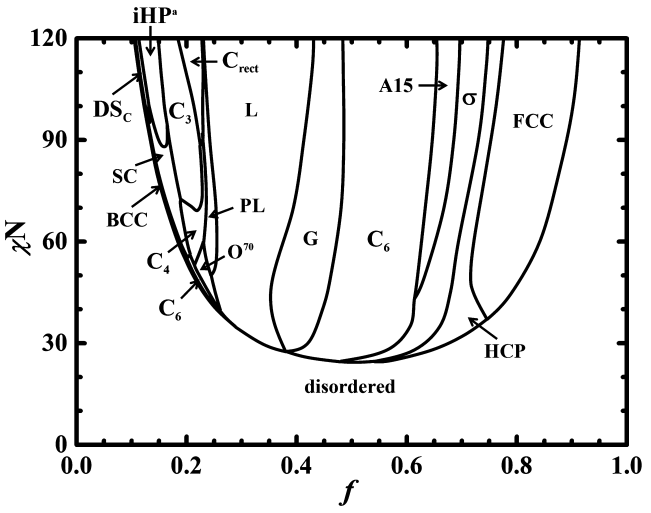

Figure 4. Phase diagram at the f–χN plane for $f_{A1} = f_{A2} = f_{A3}/2 = f/4$, $f_{B1} = f_{B2} = 0.15(1 - f)$ and $f_{B3} = 0.7(1 - f)$, that is, $\xi = \log(14/3) \approx 0.67$ and $\tau_{B2} = 0.15$.

decreasing f. As a result, the phase regions of gyroid, cylinder and sphere in the right side are widened significantly. The tendency of forming spontaneous curvature toward B-domains is mainly amplified by two effects resulting from the core–shell distribution of long B_3-block and short B_1/B_2-blocks[31] and the local branching architecture formed by the connection of A_1/A_2-blocks to B_3-block, respectively (Figure S11). In the largely expanded spherical regions, the Frank–Kasper σ and A15 phases occupy notable areas.[26,28,30] Moreover, the two nearly degenerate HCP and FCC phases replacing the classical BCC phase exhibit large windows between the σ and disordered phases.

In summary, we purposely design an AB-type block copolymer for the formation of spherical phases of low CNs. SCFT calculations demonstrate that three low-CN spherical phases, including SC, DS_C, and iHP^a, occupies a considerable stability window in the considered parameter space. We unravel that the formation of these novel phases with extremely low CNs results from the synergistic effect of the released packing frustration and the stretched bridging block. Abiding by this principle of realizing the two sophisticated mechanisms simultaneously in the same block copolymer, more multiblock copolymers can be designed for the formation of mesocrystals with low CNs. One simple example is a linear $B_1AB_2AB_3$ pentablock copolymer, where the B_2-block forms the bridging block and the lengths of B_1/B_3-blocks control the packing frustration. Therefore, this work opens a window for the design of block copolymers to expand the library of mesocrystals.

■ ASSOCIATED CONTENT

Supporting Information

The Supporting Information is available free of charge at https://pubs.acs.org/doi/10.1021/acsmacrolett.0c00313.

Self-consistent field theory (SCFT) and Figures S1–S11 (PDF)

■ AUTHOR INFORMATION

Corresponding Author

Weihua Li − *State Key Laboratory of Molecular Engineering of Polymers, Key Laboratory of Computational Physical Sciences, Department of Macromolecular Science, Fudan University, Shanghai 200433, China;* orcid.org/0000-0002-5133-0267; Email: weihuali@fudan.edu.cn

Authors

Qiong Xie − *State Key Laboratory of Molecular Engineering of Polymers, Key Laboratory of Computational Physical Sciences, Department of Macromolecular Science, Fudan University, Shanghai 200433, China*

Yicheng Qiang − *State Key Laboratory of Molecular Engineering of Polymers, Key Laboratory of Computational Physical Sciences, Department of Macromolecular Science, Fudan University, Shanghai 200433, China*

Lei Chen − *State Key Laboratory of Molecular Engineering of Polymers, Key Laboratory of Computational Physical Sciences, Department of Macromolecular Science, Fudan University, Shanghai 200433, China*

Yueming Xia − *State Key Laboratory of Molecular Engineering of Polymers, Key Laboratory of Computational Physical Sciences, Department of Macromolecular Science, Fudan University, Shanghai 200433, China*

Complete contact information is available at: https://pubs.acs.org/10.1021/acsmacrolett.0c00313

Author Contributions

‡These authors contributed equally to this work.

Notes

The authors declare no competing financial interest.

■ ACKNOWLEDGMENTS

This work was supported by National Natural Science Foundation of China (Grant Nos. 21925301 and 21774025).

■ REFERENCES

(1) Velev, O. D.; Lenhoff, A. M. Colloidal Crystals as Templates for Porous Materials. *Curr. Opin. Colloid Interface Sci.* **2000**, *5*, 56–63.

(2) von Freymann, G.; Kitaev, V.; Lotsch, B. V.; Ozin, G. A. Bottom-up Assembly of Photonic Crystals. *Chem. Soc. Rev.* **2013**, *42*, 2528–2554.

(3) O'Brien, M. N.; Jones, M. R.; Mirkin, C. A. The Nature and Implications of Uniformity in the Hierarchical Organization of Nanomaterials. *Proc. Natl. Acad. Sci. U. S. A.* **2016**, *113*, 11717–11725.

(4) Murray, C. B.; Kagan, C. R.; Bawendi, M. G. Synthesis and Characterization of Monodisperse Nanocrystals and Close-Packed Nanocrystal Assemblies. *Annu. Rev. Mater. Sci.* **2000**, *30*, 545–610.

(5) Ungar, G.; Zeng, X. B. Frank-Kasper, Quasicrystalline and Related Phases in Liquid Crystals. *Soft Matter* **2005**, *1*, 95–106.

(6) Peterca, M.; Percec, V. Recasting Metal Alloy Phases with Block Copolymers. *Science* **2010**, *330*, 333–334.

(7) Li, W. H.; Duan, C.; Shi, A.-C. Nonclassical Spherical Packing Phases Self-assembled from AB-Type Block Copolymers. *ACS Macro Lett.* **2017**, *6*, 1257–1262.

(8) Lotz, B.; Miyoshi, T.; Cheng, S. Z. D. 50th Anniversary Perspective: Polymer Crystals and Crystallization: Personal Journeys in a Challenging Research Field. *Macromolecules* **2017**, *50*, 5995–6025.

(9) Talapin, D. V. LEGO Materials. *ACS Nano* **2008**, *2*, 1097–1100.

(10) Bates, F. S.; Fredrickson, G. H. Block Copolymers - Designer Soft Materials. *Phys. Today* **1999**, *52*, 32–38.

(11) Grason, G. M. The Packing of Soft Materials: Molecular Asymmetry, Geometric Frustration and Optimal Lattices in Block Copolymer Melts. *Phys. Rep.* **2006**, *433*, 1–64.

(12) Lee, S.; Bluemle, M. J.; Bates, F. S. Discovery of a Frank-Kasper σ Phase in Sphere-Forming Block Copolymer Melts. *Science* **2010**, *330*, 349−353.
(13) Müller, M. Process-Directed Self-Assembly of Copolymers: Results of and Challenges for Simulation Studies. *Prog. Polym. Sci.* **2020**, *101*, 101198.
(14) Ungar, G.; Liu, Y. S.; Zeng, X. B.; Percec, V.; Cho, W. D. Giant Supramolecular Liquid Crystal Lattice. *Science* **2003**, *299*, 1208−1211.
(15) Zeng, X. B.; Ungar, G.; Liu, Y. S.; Percec, V.; Dulcey, A. E.; Hobbs, J. K. Supramolecular Dendritic Liquid Quasicrystals. *Nature* **2004**, *428*, 157−160.
(16) Percec, V.; Mitchell, C. M.; Cho, W. D.; Uchida, S.; Glodde, M.; Ungar, G.; Zeng, X. B.; Liu, Y. S.; Balagurusamy, V. S. K.; Heiney, P. A. Designing Libraries of First Generation AB_3 and AB_2 Self-assembling Dendrons via the Primary Structure Generated from Combinations of $(AB)_y$-AB_3 and $(AB)_y$-AB_2 Building Blocks. *J. Am. Chem. Soc.* **2004**, *126*, 6078−6094.
(17) Yu, X.; Yue, K.; Hsieh, I.-F.; Li, Y.; Dong, X.-H.; Liu, C.; Xin, Y.; Wang, H.-F.; Shi, A.-C.; Newkome, G. R.; Ho, R.-M.; Chen, E.-Q.; Zhang, W.-B.; Cheng, S. Z. D. Giant Surfactants Provide a Versatile Platform for Sub-10-nm Nanostructure Engineering. *Proc. Natl. Acad. Sci. U. S. A.* **2013**, *110*, 10078−10083.
(18) Huang, M.; Hsu, C.-H.; Wang, J.; Mei, S.; Dong, X.; Li, Y.; Li, M.; Liu, H.; Zhang, W.; Aida, T.; Zhang, W.-B.; Yue, K.; Cheng, S. Z. D. Selective Assemblies of Giant Tetrahedra via Precisely Controlled Positional Interactions. *Science* **2015**, *348*, 424−428.
(19) Yin, G.-Z.; Zhang, W.-B.; Cheng, S. Z. D. Giant Molecules: Where Chemistry, Physics, and Bio-Science Meet. *Sci. China: Chem.* **2017**, *60*, 338−352.
(20) Xie, N.; Liu, M. J.; Deng, H. L.; Li, W. H.; Qiu, F.; Shi, A. C. Macromolecular Metallurgy of Binary Mesocrystals via Designed Multiblock Terpolymers. *J. Am. Chem. Soc.* **2014**, *136*, 2974−2977.
(21) Ashcroft, N. W.; Mermin, N. D. *Solid State Physics*; Harcourt College Publishers, 1976.
(22) This interesting phase is constructively recommended by one of the reviewers.
(23) Maldovan, M.; Thomas, E. L. Diamond-Structured Photonic Crystals. *Nat. Mater.* **2004**, *3*, 593−600.
(24) Kim, J. K.; Yang, S. Y.; Lee, Y.; Kim, Y. Functional Nanomaterials Based on Block Copolymer Self-assembly. *Prog. Polym. Sci.* **2010**, *35*, 1325−1349.
(25) Orilall, M. C.; Wiesner, U. Block Copolymer Based Composition and Morphology Control in Nanostructured Hybrid Materials for Energy Conversion and Storage: Solar Cells, Batteries, and Fuel Cells. *Chem. Soc. Rev.* **2011**, *40*, 520−535.
(26) Grason, G.; DiDonna, B.; Kamien, R. Geometric Theory of Diblock Copolymer Phases. *Phys. Rev. Lett.* **2003**, *91*, 058304.
(27) Cho, B.-K.; Jain, A.; Gruner, S. M.; Wiesner, U. Mesophase Structure-Mechanical and Ionic Transport Correlations in Extended Amphiphilic Dendrons. *Science* **2004**, *305*, 1598−1601.
(28) Grason, G. M.; Kamien, R. D. Interfaces in Diblocks: A Study of Miktoarm Star Copolymers. *Macromolecules* **2004**, *37*, 7371−7380.
(29) Matsen, M. W. Effect of Architecture on the Phase Behavior of AB-Type Block Copolymer Melts. *Macromolecules* **2012**, *45*, 2161−2165.
(30) Xie, N.; Li, W. H.; Qiu, F.; Shi, A.-C. σ Phase Formed in Conformationally Asymmetric AB-Type Block Copolymers. *ACS Macro Lett.* **2014**, *3*, 906−910.
(31) Chen, L.; Qiang, Y. C.; Li, W. H. Tuning Arm Architecture Leads to Unusual Phase Behaviors in a $(BAB)_5$ Star Copolymer Melt. *Macromolecules* **2018**, *51*, 9890−9900.
(32) Lequieu, J.; Koeper, T.; Delaney, K. T.; Fredrickson, G. H. Extreme Deflection of Phase Boundaries and Chain Bridging in $A(BA')_n$ Miktoarm Star Polymers. *Macromolecules* **2020**, *53*, 513−522.
(33) Bates, M. W.; Barbon, S. M.; Levi, A. E.; Lewis, R. M.; Beech, H. K.; Vonk, K. M.; Zhang, C.; Fredrickson, G. H.; Hawker, C. J.; Bates, C. M. Synthesis and Self-Assembly of AB_n Miktoarm Star Polymers. *ACS Macro Lett.* **2020**, *9*, 396−403.
(34) Kang, C.; Kim, E.; Baek, H.; Hwang, K.; Kwak, D.; Kang, Y.; Thomas, E. L. Full Color Stop Bands in Hybrid Organic/Inorganic Block Copolymer Photonic Gels by Swelling-Freezing. *J. Am. Chem. Soc.* **2009**, *131*, 7538−7539.
(35) Segal-Peretz, T.; Winterstein, J.; Doxastakis, M.; Ramírez-Hernández, A.; Biswas, M.; Ren, J.; Suh, H. S.; Darling, S. B.; Liddle, J. A.; Elam, J. W.; de Pablo, J. J.; Zaluzec, N. J.; Nealey, P. F. Characterizing the Three-Dimensional Structure of Block Copolymers via Sequential Infiltration Synthesis and Scanning Transmission Electron Tomography. *ACS Nano* **2015**, *9*, 5333−5347.
(36) Fei, H.-F.; Li, W.; Bhardwaj, A.; Nuguri, S.; Ribbe, A.; Watkins, J. J. Ordered Nanoporous Carbons with Broadly Tunable Pore Size Using Bottlebrush Block Copolymer Templates. *J. Am. Chem. Soc.* **2019**, *141*, 17006−17014.
(37) Yi, D. H.; Nam, C.-Y.; Doerk, G.; Black, C. T.; Grubbs, R. B. Infiltration Synthesis of Diverse Metal Oxide Nanostructures from Epoxidized Diene-Styrene Block Copolymer Templates. *ACS Appl. Polym. Mater.* **2019**, *1*, 672−683.
(38) Matsen, M. W. The Standard Gaussian Model for Block Copolymer Melts. *J. Phys.: Condens. Matter* **2002**, *14*, R21−R47.
(39) Fredrickson, G. H. *The Equilibrium Theory of Inhomogeneous Polymers*; Oxford University Press: Oxford, 2006.
(40) Bates, F. S.; Hillmyer, M. A.; Lodge, T. P.; Bates, C. M.; Delaney, K. T.; Fredrickson, G. H. Multiblock Polymers: Panacea or Pandora's Box? *Science* **2012**, *336*, 434−440.
(41) Matsen, M. W.; Bates, F. S. Origins of Complex Self-assembly in Block Copolymers. *Macromolecules* **1996**, *29*, 7641−7644.
(42) Jiang, W. B.; Qiang, Y. C.; Li, W. H.; Qiu, F.; Shi, A. C. Effects of Chain Topology on the Self-assembly of AB-Type Block Copolymers. *Macromolecules* **2018**, *51*, 1529−1538.
(43) Xie, Q.; Qiang, Y. C.; Li, W. H. Regulate the Stability of Gyroids of ABC-Type Multiblock Copolymers by Controlling the Packing Frustration. *ACS Macro Lett.* **2020**, *9*, 278−283.
(44) Gao, Y.; Deng, H. L.; Li, W. H.; Qiu, F.; Shi, A. C. Formation of Nonclassical Ordered Phases of AB-Type Multiarm Block Copolymers. *Phys. Rev. Lett.* **2016**, *116*, 068304.
(45) Liu, M. J.; Qiang, Y. C.; Li, W. H.; Qiu, F.; Shi, A.-C. Stabilizing the Frank-Kasper Phases via Binary Blends of AB Diblock Copolymers. *ACS Macro Lett.* **2016**, *5*, 1167−1171.
(46) He, H. L.; Sekine, T.; Kobayashi, T. Direct Transformation of Cubic Diamond to Hexagonal Diamond. *Appl. Phys. Lett.* **2002**, *81*, 610−612.
(47) Lee, W. B.; Elliott, R.; Mezzenga, R.; Fredrickson, G. H. Novel Phase Morphologies in a Microphase-Separated Dendritic Polymer Melt. *Macromolecules* **2009**, *42*, 849−859.
(48) Matsen, M. W.; Bates, F. S. Block Copolymer Microstructures in the Intermediate-Segregation Regime. *J. Chem. Phys.* **1997**, *106*, 2436−2448.
(49) Matsen, M. W. Bridging and Looping in Multiblock Copolymer Melts. *J. Chem. Phys.* **1995**, *102*, 3884−3887.
(50) Matsen, M. W.; Thompson, R. B. Equilibrium Behavior of Symmetric ABA Triblock Copolymer Melts. *J. Chem. Phys.* **1999**, *111*, 7139−7146.

https://dx.doi.org/10.1021/acsmacrolett.0c00313
ACS Macro Lett. 2020, 9, 980−984